Supplementary Information for

Information entropy of coding metasurface

Tie Jun Cui[1,2,*] Shuo Liu[1,3], and Lian Lin Li[4]

[1] State Key Laboratory of Millimeter Waves, Southeast University, Nanjing 210096, China

[2] Cooperative Innovation Centre of Terahertz Science, No.4, Section 2, North Jianshe Road, Chengdu 610054, China

[3] Synergetic Innovation Center of Wireless Communication Technology, Southeast University, Nanjing 210096, China

[4] School of Electronics Engineering and Computer Sciences, Peking University, 100871

[*] Corresponding author. E-mail: tjcui@seu.edu.cn.

This PDF file includes:

Supplementary Text

Supplementary Figures S1 to S5

1. Coding metasurface and far electric fields

To derive the relation between the coding pattern and far-field pattern, we first consider a simple case of 1-bit coding metasurface that is located on the *xoy* plane in the Cartesian coordinate system, as shown in Supplementary Fig. S1. Then the electric current density is assumed to be uniform inside each coding particle and can be expressed as

$$\hat{J}(x,y)=\begin{cases}(\hat{x}J_x+\hat{y}J_y)e^{i\varphi_0}, & \text{For Coding 0}\\ (\hat{x}J_x+\hat{y}J_y)e^{i(\varphi_0+\pi)}, & \text{For Coding 1}\end{cases}$$

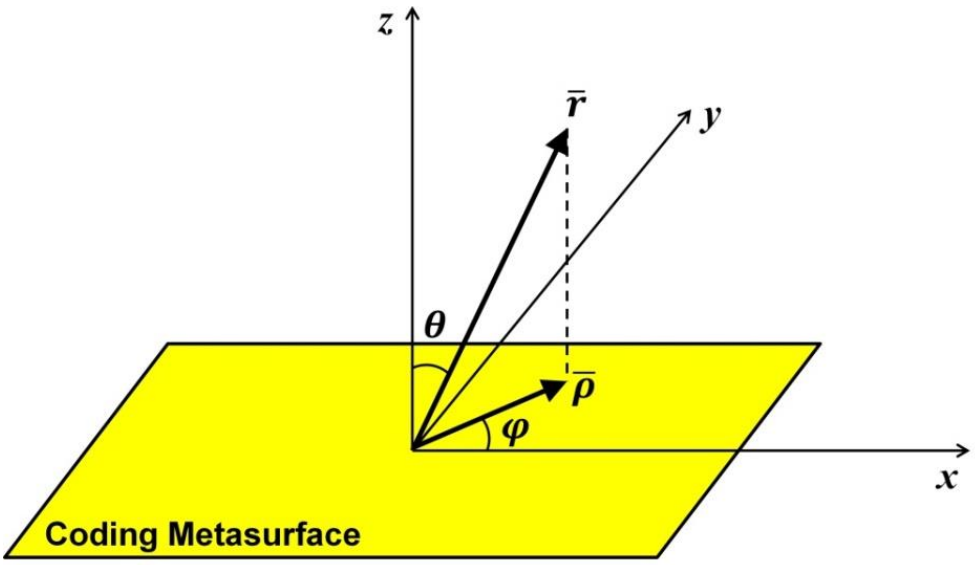

Supplementary Fig. S1. A coding metasurface located on the *xoy* plane in the Cartesian coordinate systems.

From the electromagnetic wave theory, the scattered electric field $\hat{E}^s(\bar{r})$ in the far region can be expressed by the integral of the electric current density over the entire coding metasurface with size $L_x \times L_y$ as

$$\hat{E}^s(\bar{r})=\frac{i\omega\mu_0}{4\pi}\int_{-L_x/2}^{L_x/2}dx'\int_{-L_y/2}^{L_y/2}dy'\frac{e^{ikR}}{R}\hat{J}(x',y') \tag{2}$$

in which (x',y') is the location of each coding particle on the *xoy* plane, and the distance between each coding particle to the observation point is denoted as$R=\sqrt{(x-x')^2+(y-y')^2+(z-z')^2}$. By substituting $z=rcos\theta,\ x=rsin\theta cos\varphi,\ y=rsin\theta sin\varphi, and\ z'=0$ into R and keeping the first item of its Taylor series expansion, we have

$$R=\left(r^2-2rx'sin\theta cos\varphi-2ry'sin\theta sin\varphi+x'^2+y'^2\right)^{\frac{1}{2}}$$

$$\approx r - x'sin\theta cos\varphi - y'sin\theta sin\varphi \quad (2)$$

Considering $r \gg x'sin\theta cos\varphi - y'sin\theta sin\varphi$, the item *R* in the denominator of the integral can be moved out of the integration. Substituting Eq. (2) into (1), the scattered electric field is finally written as

$$\widehat{\mathrm{E}}^{s}(r,\theta,\varphi) = \frac{i\omega\mu_0}{4\pi r} e^{ikr} \int_{-\frac{L_x}{2}}^{\frac{L_x}{2}} \int_{-\frac{L_y}{2}}^{\frac{L_y}{2}} \hat{\mathrm{J}}(x',y') e^{-i(kx'sin\theta cos\varphi + ky'sin\theta sin\varphi)} dx'dy'$$

$$= \frac{i\omega\mu_0}{4\pi r} e^{ikr} P(ksin\theta cos\varphi, ksin\theta sin\varphi)$$

in which $P(ksin\theta cos\varphi, ksin\theta sin\varphi)$ is the two-dimensional (2D) Fourier transform of the coding pattern of the metasurface.

2. Extraction of 2D polar far-field pattern

In the above section, we show that the far-field pattern is just the Fourier transform of the coding pattern. Here, we briefly introduce the processes to obtain the image of far-field pattern. **Fig. 1d** illustrates the four processes to get the image of far-field pattern in the polar coordinate system. First, the coding pattern is operated with the Fast Fourier Transform (FFT), which will generate the FFT image. However, the coordinate of the FFT image is in (*u*, *v*), in which *u* and *v* are expressed as

$$u = \frac{2\pi}{\lambda} d_x sin\theta cos\varphi \quad (1)$$

$$v = \frac{2\pi}{\lambda} d_x sin\theta sin\varphi \quad (2)$$

in which λ and d_x represent the free-space wavelength and the period of coding element, and θ and φ are the elevation and azimuthal angles in the spherical coordinate system, as shown in **Supplementary Fig. S1**. Since the maximum and minimum values of *u* and *v* are $-\pi$ and π, respectively, the coordinate transformation from (*u*, *v*) to (θ, φ) is not a bijection (one-to-one correspondence). For the coding element in this work, $\frac{2\pi}{\lambda} d_x$ equals $\frac{7\pi}{15}$, indicating that any value outside the circle with radius $\frac{7\pi}{15}$ (marked by the red circular area in **Fig. 1d**) will not be mapped to the spherical coordinate system. By transforming the coordinate inside the circular area using Eq. (1)

and (2), we obtain the 2D far-field pattern, as plotted in **Fig. 1d** (lower right), in which the horizontal and vertical axes represent the θ and φ coordinates, respectively.

Next, we further transform the data in the θ-φ Cartesian coordinate system to polar coordinate system, resulting in the image shown in the upper right in **Fig. 1d**, in which the radial and axial directions represent the θ and φ coordinates, respectively. Note that the area outside the circle is set to zero. We remark that the image of far-field pattern plotted in the 2D polar coordinate system is used to calculate the physical entropy of an encoded metasurface.

3. More results of non-periodic coding metasurfaces

Three Jerusalem-cross coding patterns and three circular-ring coding patterns are studied, in which the area of "0" coding particles increases gradually, as shown in **Supplementary Fig. S2a-c(i)** and **Fig. S3a-c(i)**, respectively. The corresponding 2D polar and 3D far-field patterns are demonstrated in **Fig. S2a-c(ii-iii)** and **Fig. S3a-c(ii-iii)**. The detailed geometrical and physical information entropies are given in **Table 1**.

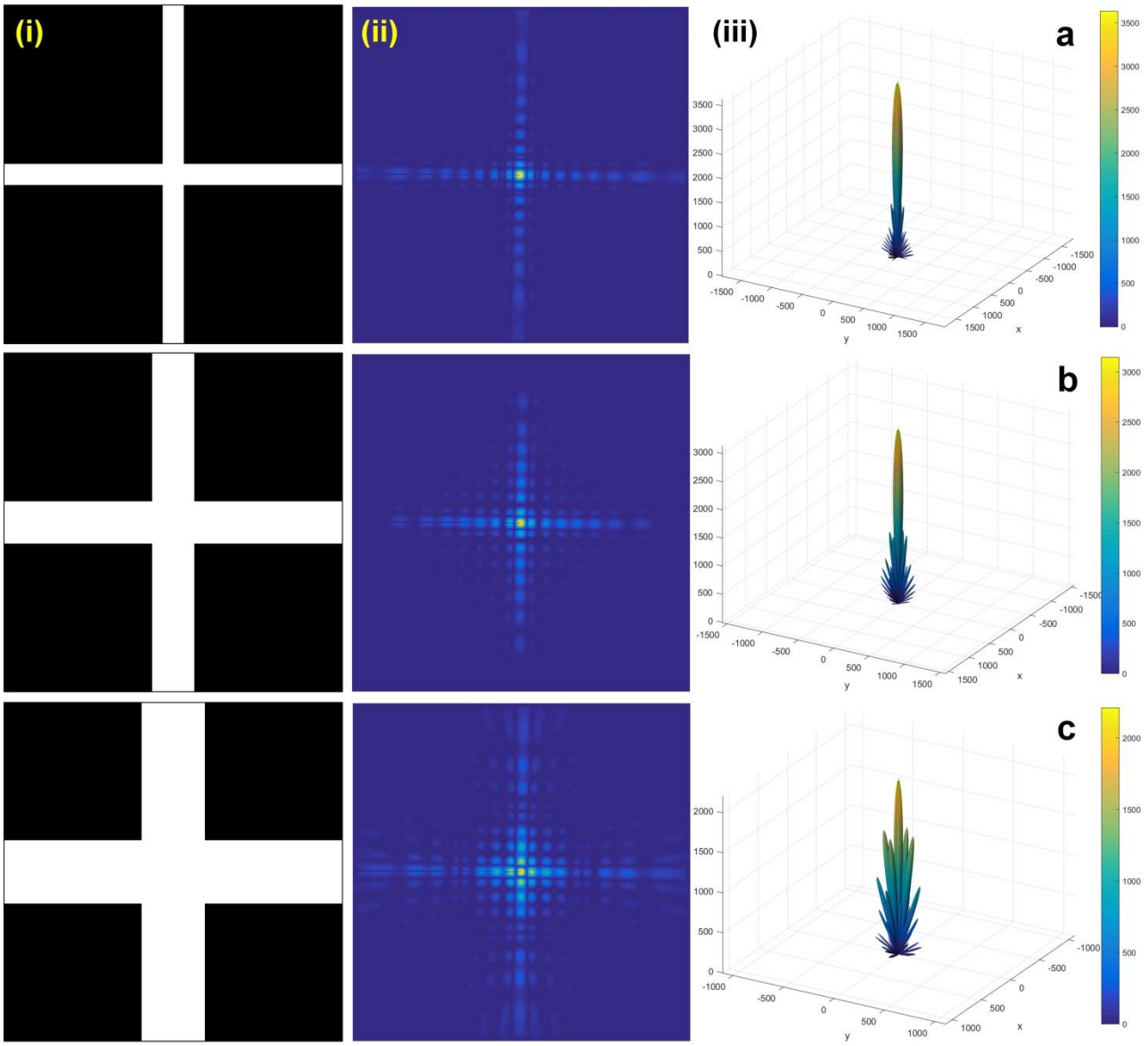

Supplementary Fig. S2. Differently-sized Jerusalem-cross coding metasurfaces and their far-field patterns. (**a**) Width of "0" particles w=4 (or 28 mm). (**b**) Width of "0" particles w=8 (or 56 mm). (**c**) Width of "0" particles w=12 (or 84 mm). (i) Coding patterns. (ii) 2D polar far-field patterns. (iii) 3D far-field patterns. Here, all three metasurfaces share the same size as 64×64 coding particles, which is equivalent to 448×448 mm^2.

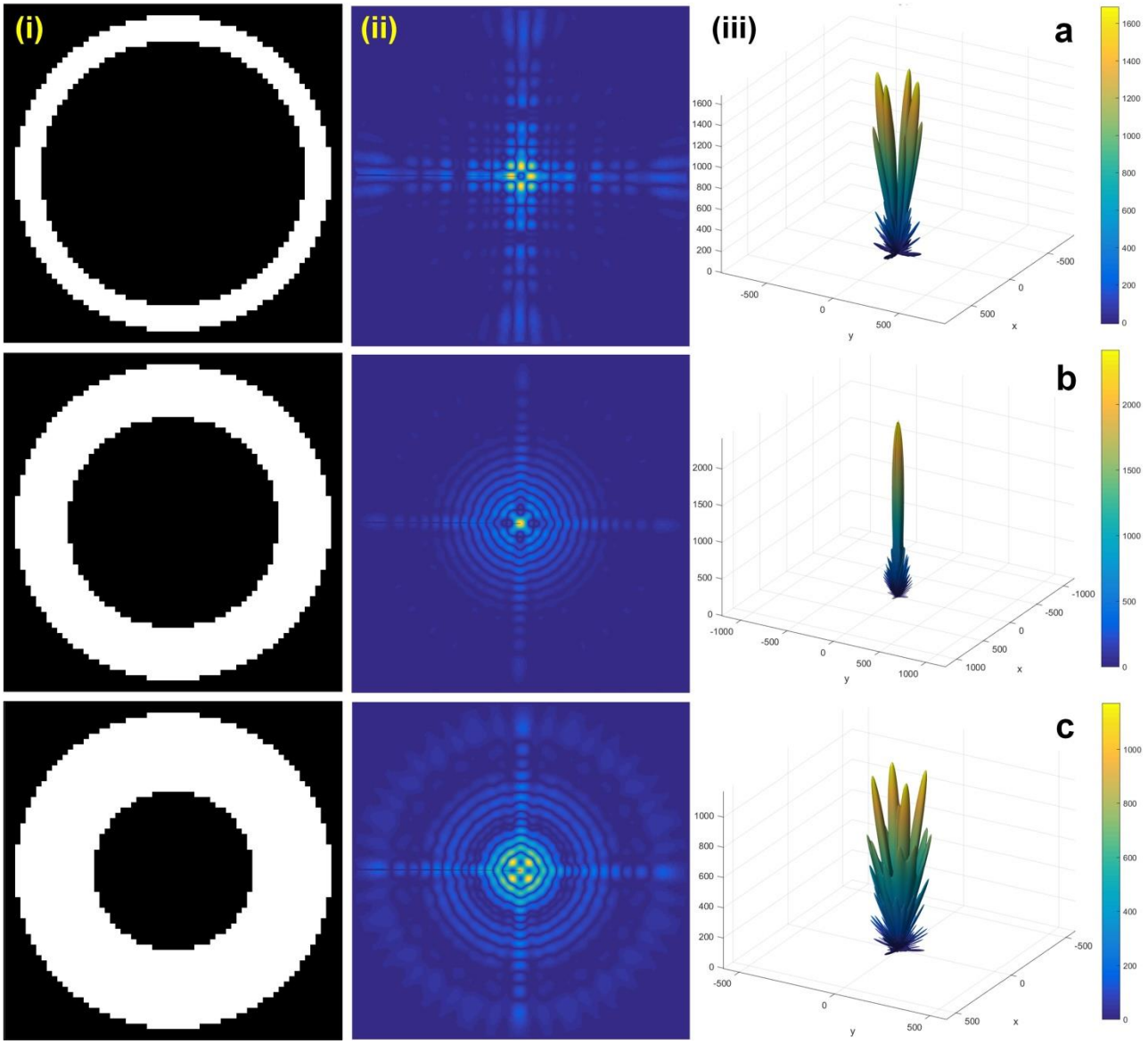

Supplementary Fig. S3. Differently-sized circular-ring coding metasurfaces and their far-field patterns. (**a**) Width of "0" particles *w*=5 (or 35 mm). (**b**) Width of "0" particles *w*=12 (or 84 mm). (**c**) Width of "0" particles *w*=15 (or 105 mm). (i) Coding patterns. (ii) 2D polar far-field patterns. (iii) 3D far-field patterns.

4. Generation of random coding metasurfaces

The generation of random coding metasurfaces is learnt from the gas molecule model. **Supplementary Fig. S4** gives a simple illustration of the entropy defined by the second law of thermodynamics. In the initial state shown in **Supplementary Fig. S4a**, two different types of gas molecules (marked by red and blue balls) with equal quantity are separated from each other in a closed

glass box. As time goes by, these two types of gas molecules gradually mix with each other due to the existence of Brownian movement of molecules, as can be observed in **Supplementary Fig. S4b**. The entropy of an isolated system, like the closed glass box, is used as a measure to predict how the dissipative process has progressed, which tends to increase over time and approaches a maximum value at equilibrium. The larger the entropy of a system, the more random of molecular chaos is. Interestingly, this diffusion process is irreversible in nature, which determines that the entropy of any isolated systems is theoretically irreducible. The random coding patterns have similar behaviors to the gas molecules.

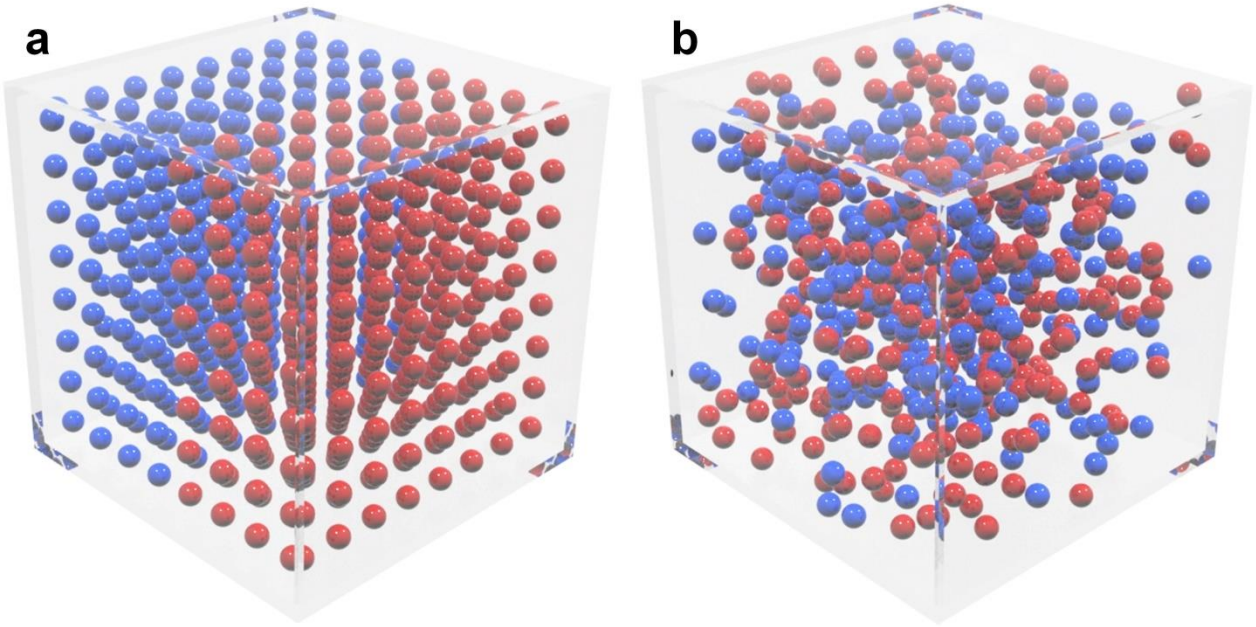

Supplementary Fig. S4. The illustration of the entropy defined by the second law of thermodynamics. (**a**) The initial state. (**b**) The steady state.

To mimic the diffusion process of gas molecules, the model of cellular automata machine is adopted to generate random coding metasurfaces in a controlled manner. **Supplementary Fig. S5** illustrates twelve random coding metasurfaces generated at the 1^{st}, 3^{rd}, 10^{th}, 20^{th}, 30^{th}, 40^{th}, 50^{th} , 60^{th}, 70^{th}, 80^{th}, 90^{th}, and 99^{th} iterations.

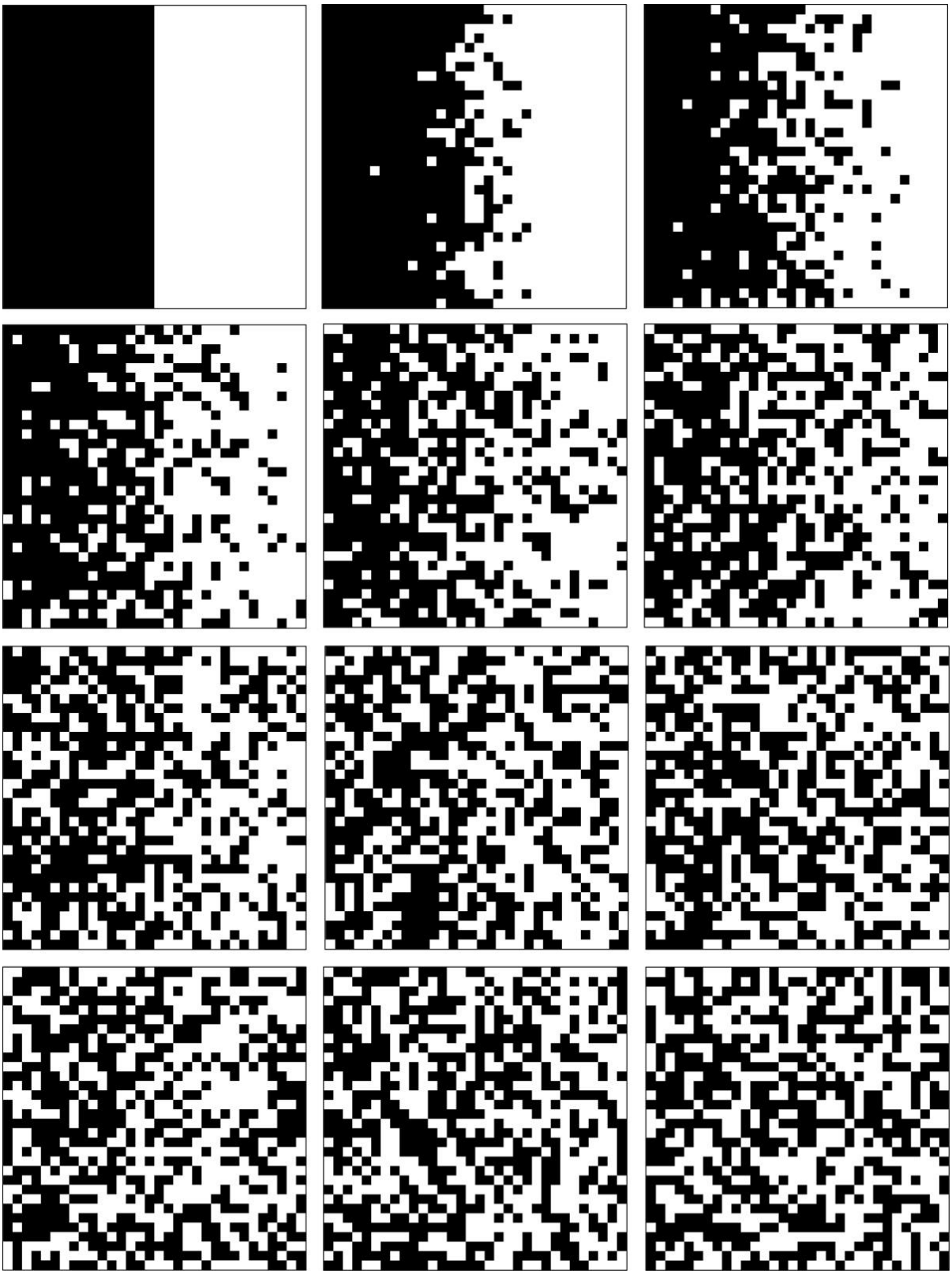

Supplementary Fig. S5. The random coding metasurfaces generated by the model of cellular automata machine at the 1st, 3rd, 10th, 20th, 30th, 40th, 50th , 60th, 70th, 80th, 90th, and 99th iterations (from the left to the right, and from the upper to the bottom orders). Each coding digit in the images includes 2×2 identical coding particles.